

Mukhtiar Singh<sup>1</sup>, Rashad Abaszade<sup>2,3</sup>, Ruslan Zapukhlyak<sup>4</sup>, Volodymyr Kotsyubynsky<sup>4</sup>,  
Fuad Abaszadeh<sup>5</sup>

## Impact of Post-Deposition Heat Treatment on the Microstructure and Mechanical Properties of Boron Nitride Thin Films Prepared by Radio Frequency Magnetron Sputtering

<sup>1</sup>*School of Mechanical Engineering, Lovely Professional University, Jalandhar-Delhi, Grand Trunk Rd, Phagwara, Punjab, India [mukhtiarts@gmail.com](mailto:mukhtiarts@gmail.com);*

<sup>2</sup>*Azerbaijan State Oil and Industry University, Baku, Azerbaijan [abaszada@gmail.com](mailto:abaszada@gmail.com);*

<sup>3</sup>*Azerbaijan University of Architecture and Construction, Baku, Azerbaijan;*

<sup>4</sup>*Vasyl Stefanyk Carpathian National University, Ivano-Frankivsk, Ukraine [volodymyr.kotsyubynsky@pnu.edu.ua](mailto:volodymyr.kotsyubynsky@pnu.edu.ua);*

<sup>5</sup>*National Aviation Academy, Baku Azerbaijan*

The effects of post-deposition heat treatment on the microstructure and mechanical properties of boron nitride thin films deposited on 316L stainless steel substrates via radio frequency magnetron sputtering were investigated. Thermal annealing procedures applied to BN coatings at 850°C within a nitrogen environment for 1.5 hours to study how heat treatment alters coating structural and functional behaviour. A systematic examination was performed to evaluate how heat treatments affected both microstructural transformations and phase compositions as well as mechanical properties. Hot treatment enhanced mechanical film properties by raising hardness values from the original 5.35 GPa in as-deposited films to 11.4 GPa alongside a clear linear thermal connection. The research shows that correct post-deposition heat treatment strengthens BN thin film structures and mechanical characteristics thus making them suitable for industrial-level applications.

**Keywords:** boron nitride, magnetron sputtering, wear resistance, surface hardness, morphology.

*Received 14 March 2025; Accepted 02 September 2025.*

## Introduction

Thin-film coatings are increasingly employed across multiple sectors to advance sustainable energy technologies, facilitate pollutant capture, and enable the fabrication of bio-compatible devices [1]. Commercial coatings typically consist of hetero-structured synthetic materials deposited onto various substrates using physical or chemical methods [2]. Such coatings offer a versatile approach to surface modification by incorporating functional external phases while preserving the bulk properties of the underlying material [3]. Optimized coating systems can simultaneously enhance chemical resistance, optical transmittance, color stability, and tribological performance of the substrate [4]. Boron nitride has emerged as a highly promising candidates for

protective steel coatings due to their exceptional mechanical and thermal properties [1]. With a hardness comparable to that of diamond and superior thermal conductivity, c-BN films provide outstanding durability under extreme operating conditions, making them suitable for applications in sustainable energy generation and advanced tribological systems [6]. Furthermore, the wide bandgap and chemical inertness of c-BN enable its integration into optical and chemically resistant devices [4]. Coating technologies encompass a broad spectrum of materials, ranging from conventional varnishes and sealants to advanced thin films and functional adhesives [7]. c-BN coatings deposited onto steel substrates significantly improve corrosion resistance and wear resistance, without altering the intrinsic mechanical characteristics of the steel matrix [3].

The synthesis and optimization of BN coatings require a detailed understanding of deposition dynamics, including temperature control, precursor flow rates, and crystallization kinetics [6]. Among the various fabrication routes, chemical vapor deposition (CVD) has established itself as the predominant technique for producing high-purity BN films with tailored crystalline phases for commercial and technological applications [7]. The ability of CVD to precisely regulate critical growth parameters allows for systematic control over film morphology, stoichiometry, and phase composition [6]. Previous studies have examined the influence of process variables on BN formation mechanisms. [5] investigated the high-temperature CVD of BN using diborane and ammonia precursors on silicon substrates, observing temperature-dependent pathways between 600–800 °C. Their work demonstrated the formation of intermediate aminodiborane species at lower temperatures and borazine at elevated temperatures, though kinetic data for the reaction pathways remained incomplete. Similarly [8] deposited BN thin films via borazine precursors in a hot-wall CVD reactor at 850–900 °C under 1 kPa, using N<sub>2</sub> as a carrier gas. Their results indicated the formation of partially ordered h-BN at 900 °C, whereas lower temperatures retained N–H bonds within the films. [9] further demonstrated that increasing diborane flow rate during CVD significantly enhanced BN film homogeneity and crystallinity at 800 °C and 267 Pa, with hydrogen dilution playing a critical role in stabilizing the coating microstructure. [10] reported on triethylboron–ammonia CVD systems at 850–1100 °C, showing a complex interplay between deposition rate, total pressure, and gas diffusivity, with turbostratic BN dominating the XRD spectra at lower temperatures. In parallel, physical vapor deposition techniques have been explored for c-BN film fabrication. [11] achieved ~500 nm c-BN coatings on 316L stainless steel via RF magnetron sputtering at room temperature, obtaining a highly crystalline phase with surface roughness below 1 nm and Vickers hardness approaching 40 GPa. [12] extended this work by incorporating a c-BN/graphite composite target at 350 °C with a -100 V substrate bias, producing 600 nm coatings with a friction coefficient of 0.2 compared to 0.7 for the bare substrate. Both studies highlighted significant improvements in wear resistance and adhesion due to the formation of dense c-BN phases.

Recent investigations using RF magnetron sputtering have emphasized the effect of plasma composition on BN film microstructure [13] demonstrated that adjusting the Ar/N<sub>2</sub> ratio during deposition on SS316L substrates strongly influenced phase evolution, with a QAr/QN<sub>2</sub> = 5/1 regime yielding the highest fraction of c-BN as confirmed by XRD and FTIR analyses. Complementary post-deposition annealing studies further showed that thermal activation between 800 °C and 1000 °C promoted wurtzite BN (w-BN) formation and significantly enhanced hardness from about 5 GPa to over 11 GPa, confirming the role of heat treatment in phase stabilization and mechanical performance optimization.

## I. Experimental details

In the present study, cubic boron nitride (c-BN) thin films were deposited onto SS316L stainless steel substrates using the radio frequency (RF) magnetron sputtering technique. Prior to deposition, all specimens underwent surface preparation involving ultrasonic cleaning in a petroleum ether solution for 3 minutes, followed by rinsing in deionized water to remove residual contaminants and ensure optimal adhesion. The experimental configuration is illustrated in Figure 1, featuring a high-vacuum deposition chamber with an internal diameter of 330 mm. The system was equipped with a balanced plane magnetron and an electron beam source, enabling precise control of plasma parameters during film growth.

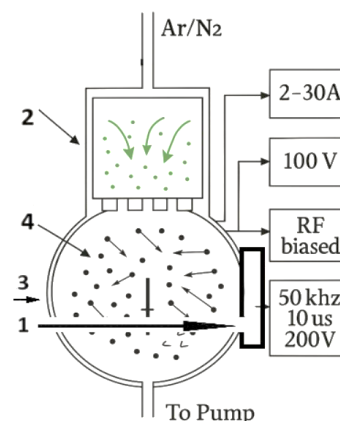


**Fig. 1.** The experimental setup: 1 – magnetron, 2 – source of electron. 3 – gas chamber, 4 – specimens.

The deposition chamber was equipped with a balanced plane magnetron (1) and a broad electron beam source (2) with an active surface area of 50 cm<sup>2</sup> (Figure 1). For sputtering, an 80 mm diameter, 10 mm thick hexagonal boron nitride (h-BN) target with 99.9% purity was mounted on a water-cooled magnetron gun and connected to a 13.56 MHz RF generator via a matching network. The h-BN target was sputtered in RF mode at a discharge power of 150 W. The auxiliary electron source operated using a titanium nitride hollow cathode, with discharge currents 2–20 A and voltages adjusted from 300 V to 25 V. During deposition the electron beam energy was maintained at 100 eV.

SS316L stainless steel substrates (15 mm × 10 mm) were mechanically polished and ultrasonically cleaned in acetone prior to loading. The chamber was evacuated to a base pressure of 10<sup>-6</sup> Torr using a turbomolecular pumping system. Pre-deposition ion etching was conducted in Ar plasma with an ion current density of 2 mA cm<sup>-2</sup> and a pulsed bias of 500 V (50 kHz, 12.5 μs) to ensure surface activation. During film growth, the substrate bias was maintained at 200 V.

Reactive sputtering was performed using mixed Ar/N<sub>2</sub> atmospheres at three different flow regimes: QAr/QN<sub>2</sub> = 5/1, 5/2.5, and 1/5. These conditions produced three distinct coating sets, designated as BN1, BN2, and BN3, respectively. The total working pressures were controlled within 0.7–5 Torr for BN1, 0.5–6 Torr for BN2,

and 0.5–5 Torr for BN3. These variations in Ar/N<sub>2</sub> ratio were designed to investigate the influence of plasma composition on phase formation and microstructural evolution of the c-BN thin films. To evaluate the effect of thermal processing on phase evolution and mechanical performance, post-deposition heat treatments were applied to the c-BN thin films. Annealing was carried out in a controlled nitrogen atmosphere at temperatures of 850 °C for 1.5 hours. Following deposition, the coated specimens were sectioned using a diamond saw to ensure minimal mechanical stress on the films. The cross-sectional samples were embedded in epoxy resin for cold mounting to preserve the integrity of the coating–substrate interface. Polishing was performed using progressively finer grades to obtain a defect-free surface suitable for microstructural examination. Metallurgical characterization of the prepared cross-sections was conducted using a combination of optical microscopy, X-ray diffraction (XRD), and field emission scanning electron microscopy (FE-SEM). This integrated approach allowed for comprehensive analysis of the coating morphology, phase composition, and the quality of the interface between the BN film and SS316L substrate.

XRD analysis (Bruker AXS diffractometer 1°/min speed over  $2\theta = 10^\circ$ – $100^\circ$ , 40 kV/40 mA Cu-K radiation) was performed to determine the crystalline phases present in the BN films and to monitor phase evolution under different deposition regimes and post-deposition annealing. FE-SEM (JSM-7610F FESEM) was used for imaging of surface morphology and grain structure. Elemental composition and B/N ratios were assessed using EDS coupled with SEM. Adhesion strength of the coatings was evaluated via progressive-load scratch tests using a Rockwell indenter. Mechanical performance of the BN thin films was assessed by nanoindentation to measure hardness and elastic modulus. The method provided quantitative correlation between deposition parameters, phase composition, and mechanical strengthening following annealing.

## II. Results and Discussion

XRD patterns of as-deposited boron nitride film

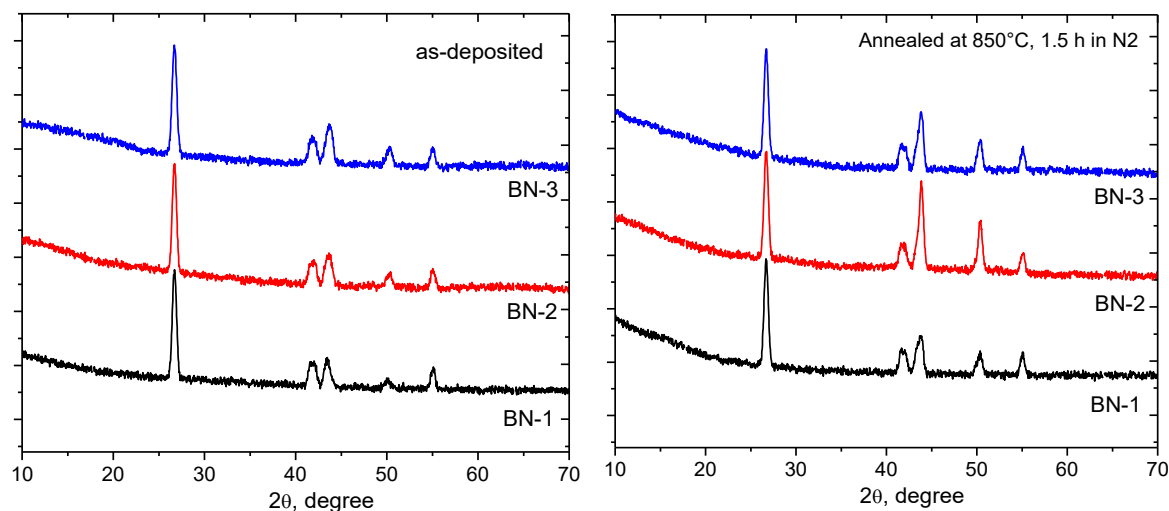


**Fig. 2.** XRD patterns of as-deposited (a) and annealed at 850°C in N<sub>2</sub> (b) boron nitride thin film obtained at regimes BN1, BN2, BN3.

(Fig.2, a) obtained at different regimes (BN1, BN2, BN3) correspond a presence of layered BN phases (rhombohedral/orthorhombic polytypes) and a minor cubic-ordered component. All patterns exhibit broad reflections (FWHM  $\approx 0.5$ – $0.6^\circ$ ) indicative of limited coherent domain size and microstrain in the as-deposited state. Strong, broad basal reflection observed for BN1 sample at  $26.7^\circ$  is assigned to the (002)/(003) of the layered structure, accompanied by weak peaks in the  $41.6$ – $43.6^\circ$  range that correspond to in-plane (100)/(101)-type reflections of layered BN with overlap from orthorhombic (020)/(200)). The peaks of c-BN are observed at  $43.9^\circ$  ((111)) and  $50.4^\circ$  ((200)). For BN2 sample the region around  $43$ – $44^\circ$  has two-component shape due a contribution of (101) peak layered-BN and (111) peak of c-BN, signaling a higher cubic content while the basal layered peak remains broad, consistent with turbostratic stacking disorder. The c-BN (111) and (200) peaks at  $43.9^\circ$  and  $50.4^\circ$ , respectively are clearly visible when the layered BN basal peak at  $26.7^\circ$  is still present but reduced in relative intensity, and the the  $42$ – $45^\circ$  region reflects overlap between layered-BN (100/101) and c-BN(111). Peak broadening are comparable to BN1 and BN2 samples, indicating that the enhanced c-BN fraction arises predominantly from changes in phase composition rather than crystallite growth. Post-deposition thermal treatment of the BN coatings resulted in significant improvements in phase stability and crystalline order (Fig.2, b). Thermal activation facilitated the transformation towards the cubic boron nitride (c-BN) phase, with diffraction peaks exhibiting increased intensity and reduced full-width at half-maximum (FWHM), indicative of enhanced crystallinity. The BN-2 samples demonstrated pronounced peak intensities at  $2\theta = 44.36^\circ$  and  $52.41^\circ$ , confirming a higher phase purity of c-BN. For BN-3 coatings, post-annealing induced structural reordering and stress relaxation, which manifested as a reduction in turbostratic and amorphous BN contributions. The BN-1 films, initially dominated by orthorhombic and rhombohedral BN phases, also exhibited a notable increase in c-BN content following heat treatment. This phase redistribution was accompanied by improved hardness and thermal stability, suggesting a strong correlation between annealing-induced

crystallization and mechanical performance. The observed enhancement in c-BN fraction across all regimes confirms the critical role of post-deposition heat treatment in driving phase transformation and optimizing functional properties. These findings are consistent with previous reports on stress-assisted nucleation of c-BN and demonstrate the suitability of thermally treated BN coatings for demanding high-temperature and wear-resistant applications.

The microstructural evolution of boron nitride thin films under post-deposition annealing was examined using FE-SEM. In the BN1 regime (Figure 3a), annealing induced noticeable grain refinement and morphological changes consistent with a phase transformation towards the wurtzite BN (w-BN) structure. The emergence of w-BN in this regime is associated with enhanced hardness, corroborating the mechanical testing results. For the BN2 coatings (Figure 3b), post-heat treatment resulted in a more distinct development of well-crystallized w-BN grains.

The increased ordering of the microstructure is directly linked to the improved surface hardness observed after annealing, highlighting the effect of thermal activation on phase stabilization. In the BN3 regime (Figure 3c), the SEM and corresponding EDS analyses revealed a highly refined grain structure with enhanced crystallinity, further supporting the transformation towards the w-BN phase. The micrographs displayed increased grain cohesion and reduced porosity; indicative of densification driven by thermally activated diffusion mechanisms. Such structural consolidation promotes grain boundary strengthening and defect minimization, producing a compact, high-purity coating. The formation of the w-BN phase across all regimes positions these coatings as promising candidates for high-temperature tribological systems and protective applications requiring high hardness and thermal stability.

Cross-sectional SEM analysis provided further insight into the coating morphology under different deposition regimes (Figure 3 d,e,f). The BN3 regime (Figure 3f)

exhibited a non-uniform surface characterized by a dendritic growth pattern with branching, tree-like structures. Such morphology is indicative of rapid nucleation and anisotropic grain growth, commonly associated with kinetic limitations during film deposition. The larger average grain size observed in BN3 suggests the presence of fewer but coarser grains, which can significantly influence the mechanical response by altering hardness and wear resistance. In contrast, the BN2 coatings (Figure 3e) displayed a comparatively smoother and more homogeneous microstructure with refined grains, reflecting a more controlled growth process and improved film uniformity. The BN1 coatings exhibited irregular morphologies (Figure 3d), with pronounced dendritic features, suggesting a distinct but still non-uniform grain formation mechanism under this sputtering regime.

Grain size plays a critical role in determining the functional performance of BN thin films. The presence of larger grains, as observed in BN3, may enhance thermal stability but can reduce hardness and increase susceptibility to wear due to lower grain boundary density. The finer and more uniform microstructure in BN2 supports improved mechanical strength and wear resistance, correlating with the superior hardness and adhesion values obtained for this regime.

Adhesion performance of the BN thin films was evaluated using progressive-load scratch testing with a Rockwell indenter of 200  $\mu\text{m}$  tip radius. The tests were conducted at a constant sliding speed of 3  $\text{mm min}^{-1}$  while incrementally increasing the normal load. Acoustic emission monitoring and in-situ friction force measurements were performed simultaneously to accurately identify the critical load corresponding to coating delamination. Microscopic inspection of the scratch tracks provided corroborative evidence for failure initiation and coating detachment.

Among the investigated regimes, the BN2 coatings exhibited superior adhesion, with minimal delamination

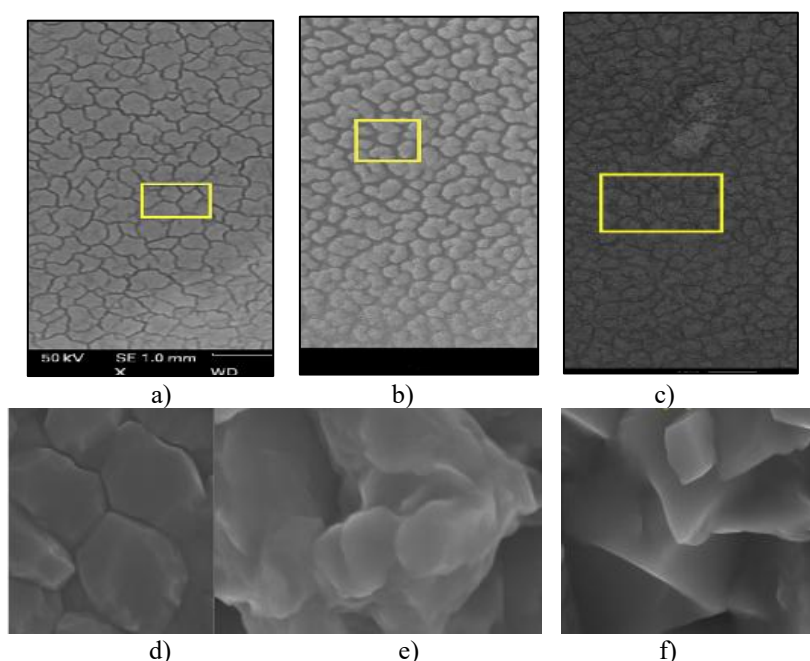
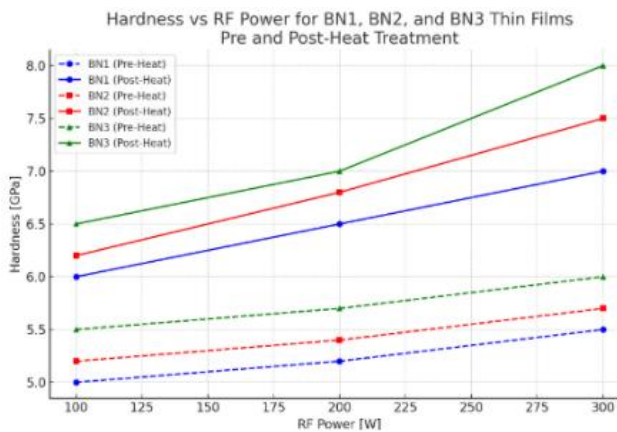


**Fig. 3.** SEM images of boron nitride thin film obtained at regimes (a) BN1, (b) BN2, and (c) BN3.



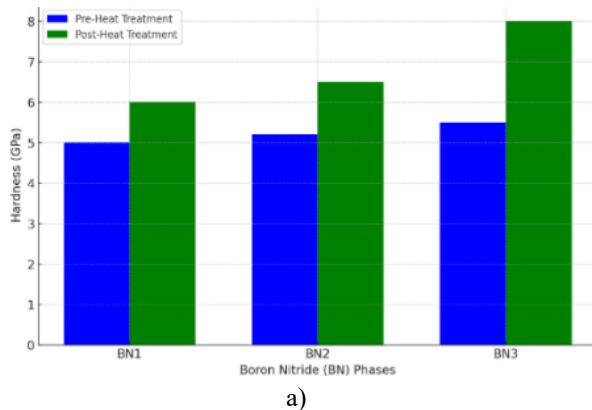
observed along the scratch path and an average critical load of 126 N. The elastic recovery behavior noted around the indenter track suggested that the coating resisted plastic deformation under increasing load, indicating a strong interfacial bond. In contrast, the BN1 and BN3 coatings showed earlier failure, with critical loads of approximately 102 N and 96 N, respectively, and clear signs of coating detachment along the wear path. The enhanced adhesion strength of the BN2 films is attributed to their denser microstructure and higher fraction of c-BN phase, which promotes stronger coating–substrate interaction and improved load-bearing capacity. These findings align with the observed microstructural uniformity of BN2 and confirm its suitability for applications demanding high mechanical integrity and wear resistance.

A comparative analysis of nanoindentation measurements (Fig. 4) demonstrated that post-deposition heat treatment significantly affected the hardness of BN-1, BN-2, and BN-3 thin films by altering their phase composition and microstructural characteristics. The BN-1 coatings, primarily composed of hexagonal boron nitride (h-BN), exhibited the lowest baseline hardness of approximately 5 GPa.



**Fig. 4.** Variation of hardness as a function of RF power for BN1, BN2, and BN3 thin films in the as-deposited state and after post-deposition heat treatment.

This behavior is attributed to the layered structure of h-BN, where weak interlayer van der Waals forces facilitate slip under applied stress, resulting in reduced resistance to deformation. In contrast, BN-2 films



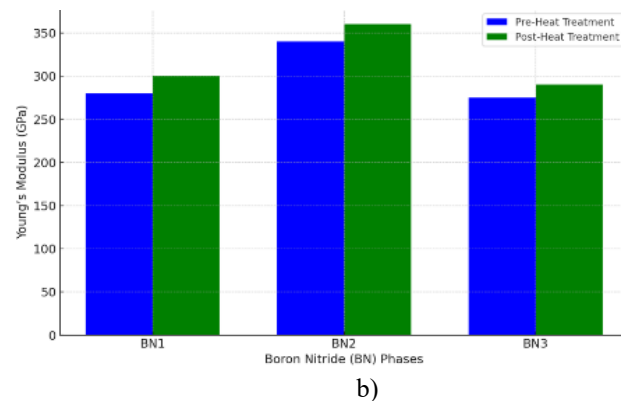
displayed a slightly higher as-deposited hardness (about 5.2 GPa), reflecting their denser bonding network and improved structural integrity relative to BN-1. The BN-3 coatings demonstrated the highest initial hardness of approximately 5.5 GPa due to their microstructure approaching that of cubic boron nitride (c-BN), whose three-dimensional covalent bonding network is known for exceptional mechanical strength.

Figure 5 demonstrates Nano-hardness values of BN-1, BN-2, and BN-3 thin films in the as-deposited condition and after post-deposition heat treatment. The results demonstrate a consistent increase in hardness across all regimes following annealing, with BN-3 exhibiting the highest absolute values due to extensive c-BN phase formation and microstructural densification. The elastic modulus and nano-hardness of the BN thin films were evaluated using a NanoAnalyzer equipped with a high bending rigidity cantilever, enabling precise measurements within a stiff contact regime. Nano-hardness was determined using a sclerometric technique, in which uniform scratches were produced under controlled loading conditions, and the standard widths of the scratches were analyzed. A calibration curve generated from a reference material with a known nano-hardness value was used to ensure measurement accuracy.

The applied scratching loads ranged from 700 N to 3600 N, while the average scratch depth was maintained below 155 nm to minimize substrate effects and ensure that the measurements reflected only the coating properties. Elastic modulus determination was performed via a point-wise approach curve analysis at multiple test points.

During the measurement, the probe established initial contact with the film surface, and the resulting frequency shifts from elastic repulsion forces were recorded. The slope of the approach curves, directly related to the contact stiffness, was used to calculate the elastic modulus of the BN coatings. This methodology enabled accurate mechanical characterization of ultra-thin layers down to 1 nm thickness. The combined nano-hardness and elastic modulus data provided critical insights into the correlation between microstructural evolution, phase composition, and mechanical performance of the BN coatings (Figure 5b).

The incorporation of cubic boron nitride (c-BN) within the coatings plays a pivotal role in enhancing their mechanical properties, as c-BN is one of the hardest



**Fig. 5.** (a) Nano-hardness and (b) Young's modulus values of BN-1, BN-2, and BN-3 thin films before and after post-deposition heat treatment.

known materials. The formation of this metastable phase in the BN-2 regime is closely linked to the generation of high compressive stress during deposition. Such stress induces lattice distortion, which thermodynamically favors nucleation and stabilization of the c-BN phase. The Young's modulus values obtained from approach curve analysis further confirmed the presence of c-BN in the films. Since Young's modulus is a direct measure of material stiffness, the observed increase in modulus for c-BN-rich coatings correlate with their higher hardness and improved wear resistance compared to non-c-BN films. The relationship between compressive stress and c-BN content explains why the BN-2 coatings, deposited under optimized Ar/N<sub>2</sub> ratios, exhibited both the highest modulus and hardness values. As shown in Figure 5b, the as-deposited Young's modulus values for BN-1, BN-2, and BN-3 were approximately 280 GPa, 340 GPa, and 275 GPa, respectively, reflecting their intrinsic phase compositions. Post-deposition heat treatment further increased the modulus to 300 GPa for BN-1, 360 GPa for BN-2, and 290 GPa for BN-3. These enhancements are attributed to thermally induced phase stabilization and improved bonding, particularly the increased formation of c-BN in BN-2. The parallel rise in both stiffness and hardness highlights the strong structure-property correlation and demonstrates that compressive stress engineering combined with thermal activation is an effective route for optimizing BN thin film performance. The friction coefficient (FC) measurements (Figure 6) for BN-1, BN-2, and BN-3 thin films deposited on SS316L substrates revealed significant differences in tribological performance before and after post-deposition heat treatment. The BN-1 coatings, dominated by hexagonal boron nitride (h-BN), exhibited the highest initial FC values. This behavior reflects the intrinsic characteristics of the layered h-BN structure, where weak interlayer van der Waals forces lead to easier shear and higher susceptibility to wear under mechanical stress. Progressive testing showed an increase in friction over time, indicating accelerated surface degradation. Post-annealing, BN-1 demonstrated only a marginal reduction in frictional instability, suggesting that while phase stabilization occurred, the persistence of the soft h-BN phase continued to limit wear resistance.

In contrast, the BN-2 films, enriched with cubic boron nitride (c-BN), exhibited the lowest FC values both in the as-deposited and annealed states. The stable and minimal friction response observed during testing is attributed to the higher hardness and structural integrity imparted by the c-BN phase, which offers superior resistance to sliding-induced damage. The BN-3 coatings, comprising a mixed h-BN/c-BN phase composition, demonstrated intermediate tribological behavior, with better wear resistance than BN-1 but not matching the performance of BN-2. Post-deposition annealing improved the overall wear resistance of all coatings, with the BN-2 regime showing the most significant benefit due to increased c-BN phase content and microstructural densification. These results confirm that thermal treatment enhances the tribological stability of BN coatings, and they highlight the critical role of c-BN formation in reducing friction and improving long-term performance in demanding mechanical environments. Post-deposition heat treatment

produced significant variations in the tribological response of BN-1, BN-2, and BN-3 thin films deposited on SS316L substrates. The BN-1 coatings, dominated by hexagonal boron nitride (h-BN), exhibited the highest wear rates after annealing.

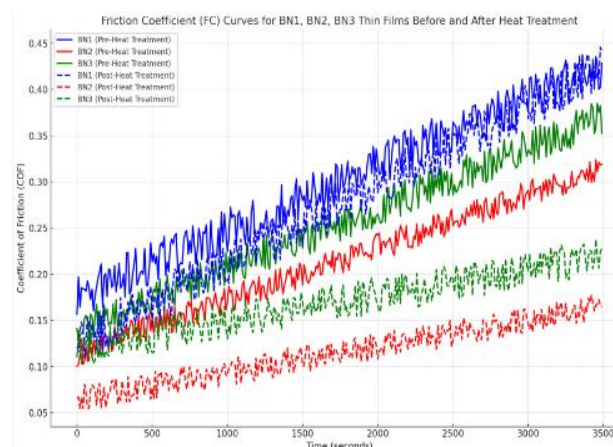


**Fig. 6.** Tribological testing of BN thin films using a 52100 steel ball under a 70 g load at a sliding speed of 1.54 cm s<sup>-1</sup>.

SEM examination (Figure 7a) revealed extensive surface damage, including deep grooves, craters, and pronounced ploughing, indicative of severe material pull-out. This behavior reflects the intrinsic softness and weak interlayer bonding of h-BN, which facilitates shear and accelerates wear under sliding contact. In contrast, BN-2 films, enriched with c-BN, demonstrated exceptional wear resistance following heat treatment. SEM analysis (Fig. 7b) showed only minor abrasion and faint ploughing marks, with no evidence of material transfer or deep groove formation. The improved tribological performance is attributed to the increased c-BN phase fraction, which enhances hardness, load-bearing capacity, and surface integrity. The BN-3 coatings, comprising a mixed h-BN/c-BN phase composition, exhibited intermediate behavior (Fig. 7, c). While moderate abrasion, cratering, and pitting were observed, the presence of c-BN reduced the extent of material removal compared to BN-1.

The dual-phase structure likely moderates friction and wear by combining the lubricating properties of h-BN with the mechanical robustness of c-BN. Post-annealing observations underscore the critical role of the c-BN phase in improving tribological performance. The BN-2 regime, which achieved the highest c-BN content and structural densification after heat treatment, consistently demonstrated superior wear resistance, confirming the strong correlation between phase composition and mechanical durability in BN thin films.

## Conclusions

The post-deposition heat treatment had a pronounced effect on the structural, mechanical, and tribological behavior of BN-1, BN-2, and BN-3 thin films deposited on 316L stainless steel substrates. In their as-deposited state, BN-1 coatings, dominated by hexagonal boron nitride (h-BN), exhibited the lowest hardness and poorest wear resistance due to the intrinsic softness of the layered

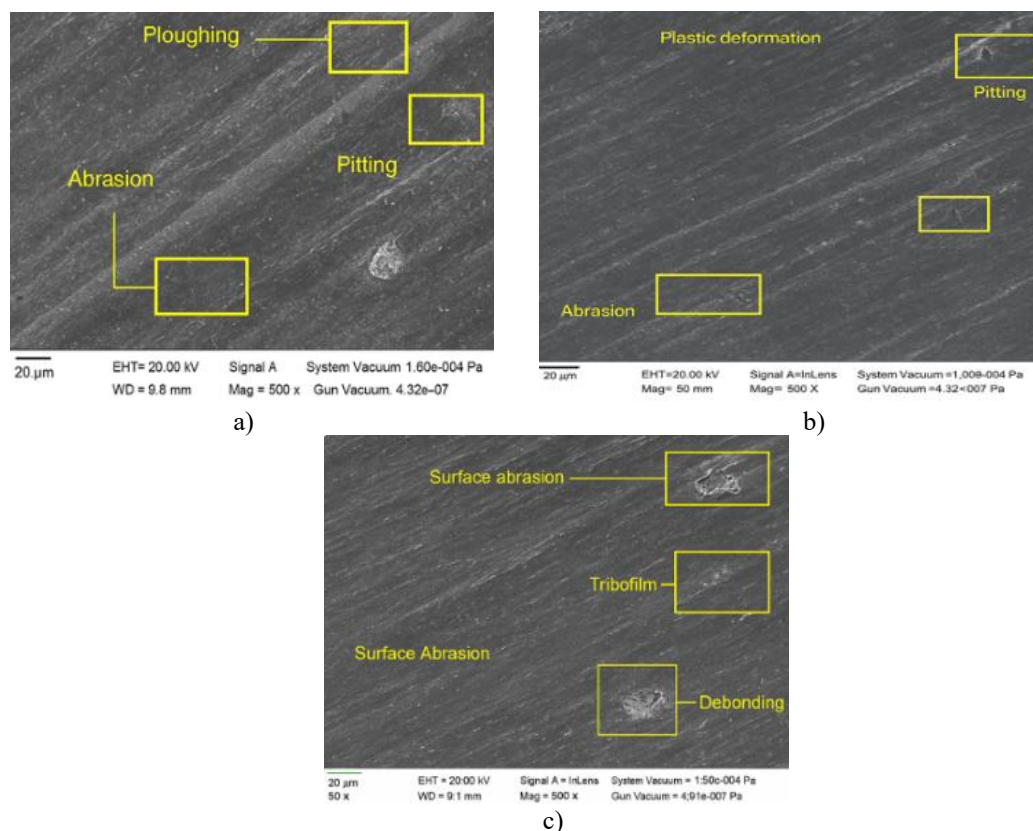


**Fig. 7.** Typical post-heat-treated SEM images of the worn surfaces of BN-coated SS316L substrates: (a) BN-1 (b) BN-2, (c) BN-3.

h-BN structure. Thermal annealing improved phase stability and increased hardness; however, the wear resistance of BN-1 remained inferior compared to the other regimes because of the persistent h-BN fraction. BN-2 coatings demonstrated the most favorable performance. The higher content of cubic boron nitride (c-BN) contributed to medium baseline hardness in the as-deposited state, which further increased significantly upon annealing at 1000 °C. The enhanced c-BN phase fraction resulted in superior hardness, minimal friction, and outstanding wear resistance, highlighting BN-2 as the most mechanically robust coating. BN-3 films, containing a mixed h-BN/c-BN phase composition, exhibited intermediate properties. Although as-deposited wear resistance exceeded that of BN-1, it remained below BN-2. Post-heat treatment promoted further c-BN formation and hardness enhancement; however, residual h-BN

inclusions limited their tribological performance relative to BN-2. These findings confirm that post-deposition heat treatment is an effective strategy for improving the structural and functional properties of BN thin films. The BN-2 regime, with its optimized c-BN content and high mechanical performance, emerges as the most promising candidate for high-performance industrial applications requiring enhanced durability, hardness, and wear resistance.

**Singh Mukhtiar** – PhD, Associate Professor;  
**Abaszade R.G.** – PhD, Associate Professor;  
**Zapukhlyak Ruslan** – PhD, Associate Professor;  
**Kotsyubynsky Volodymyr** – Professor, Doctor of Sciences;  
**Abaszadeh Fuad** – PhD.

- [1] R. Ananthakumar, B. Subramanian, A. Kobayashi, M. Jayachandran, *Electrochemical corrosion and materials properties of reactively sputtered TiN/TiAlN multilayer coatings*, *Ceramics International*, 38(1), 477 (2012); <https://doi.org/10.1016/j.ceramint.2011.07.030>.
- [2] K. Mech, R. Kowalik, P. Żabiński, *Cu thin films deposited by DC magnetron sputtering for contact surfaces on electronic components*, *Archives of Metallurgy and Materials*, (2011).
- [3] Y.H. Zhao, L. Hu, G.Q. Lin, J.Q. Xiao, C. Dong, B.H. Yu, *Deposition, microstructure and hardness of TiN/(Ti,Al)N multilayer films*, *International Journal of Refractory Metals and Hard Materials*, 32, 27-32 (2012). <https://doi.org/10.1016/j.ijrmhm.2012.01.003>.
- [4] A.O. Mateescu, G. Mateescu, M. Balasoiu, G.O. Pompilian, M. Lungu, *Coating multilayer material with improved tribological properties obtained by magnetron sputtering*, *IOP Conference Series: Materials Science and Engineering*, 174, 012059 (2017); <https://doi.org/10.1088/1757-899X/174/1/012059>.
- [5] C. Navas, R. Colaço, J. de Damborenea, R. Vilar, *Abrasive wear behaviour of laser clad and flame sprayed-melted NiCrBSi coatings*, *Surface and Coatings Technology*, 200(24), 6854 (2006); <https://doi.org/10.1016/j.surfcoat.2005.10.032>.



- [6] D.E.N.G. Bin, T.A.O. Ye, Zhijie H.U., *The microstructure, mechanical and tribological properties of TiN coatings after Nb and C ion implantation*, Applied Surface Science, 284, 405 (2013).
- [7] C.D. Rivera-Tello, E. Broitman, F.J. Flores-Ruiz, O. Jiménez, M. Flores, *Mechanical properties and tribological behavior at micro and macro-scale of WC/WCN/W hierarchical multilayer coatings*, Tribology International, 101, 194 (2016); <https://doi.org/10.1016/j.triboint.2016.04.017>.
- [8] J.T. Gudmundsson, A. Anders, A. von Keudell, *Foundations of physical vapor deposition with plasma assistance*, Plasma Sources Science and Technology, 31(8), 083001 (2022); <https://doi.org/10.1088/1361-6595/ac7f53>.
- [9] M.A. Lieberman, A.J. Lichtenberg, *Principles of Plasma Discharges and Materials Processing*, 2nd Edition, John Wiley & Sons, Inc., New York (2005). ISBN: 978-0-471-72425-4.
- [10] M. Ohring, *Materials science of thin films: deposition and structure*, Academic Press Inc., San Diego (2002). <https://doi.org/10.1016/B978-0-12-524975-1.X5000-9>.
- [11] F. Zhou, K. Adachi, K. Kato, *Influence of deposition parameters on surface roughness and mechanical properties of boron carbon nitride coatings synthesized by ion beam assisted deposition*, Thin Solid Films, 497(1–2), 210 (2006); <https://doi.org/10.1016/j.tsf.2005.10.070>.
- [12] M. Singh, H. Vasudev, & R. Kumar, *Microstructural characterization of BN thin films using RF magnetron sputtering method*. Materials Today: Proceedings, 26(2), 2277 (2020); <https://doi.org/10.1016/j.matpr.2020.02.211>.

Мухтіар Сінгх<sup>1</sup>, Рашад Абасзаде<sup>2,3</sup>, Руслан Запыхляк<sup>4</sup>, Володимир Коцюбинський<sup>4</sup>,  
Фуад Абасзаде<sup>5</sup>

## Вплив термообробки на мікроструктуру та механічні властивості тонких плівок нітриду бору, отриманих методом радіочастотного магнетронного розпилення

<sup>1</sup>Школа машинобудування, Lovely Professional University, Джаландхар–Делі, Grand Trunk Rd, Пхазгара, Пенджаб, Індія, [mukhtiarts@gmail.com](mailto:mukhtiarts@gmail.com)

<sup>2</sup>Азербайджанський державний нафтогазовий та промисловий університет, Баку, Азербайджан, [abaszada@gmail.com](mailto:abaszada@gmail.com)

<sup>3</sup>Азербайджанський університет архітектури та будівництва, Баку, Азербайджан

<sup>4</sup>Карпатський національний університет імені Василя Стефаника, Івано-Франківськ, Україна, [volodymyr.kotsuybynsky@pnu.edu.ua](mailto:volodymyr.kotsuybynsky@pnu.edu.ua)

<sup>5</sup>Національна авіаційна академія, Баку, Азербайджан

У дослідженні розглянуто вплив термообробки на мікроструктуру та механічні властивості тонких плівок нітриду бору, осаджених на підкладки з нержавіючої сталі 316L методом радіочастотного магнетронного розпилення. Термічний відпал проводили при температурі 850 °C протягом 1,5 години в атмосфері азоту для оцінки впливу контрольованого нагріву на структурні та функціональні характеристики покриттів. Комплексна характеристика дозволила дослідити еволюцію фаз, мікроструктурні перетворення та механічну поведінку плівок. Було встановлено, що відпал призвів до суттєвого покращення механічних властивостей: твердість зросла з 5,35 ГПа для вихідних зразків до 11,4 ГПа. Отримані результати доводять, що оптимально підібраний режим термообробки підвищує фазову стабільність, щільність та механічну цілісність покриттів BN, що робить їх придатними для використання у промислових застосуваннях.

**Ключові слова:** нітрид бору, магнетронне розпилення, зносостійкість, твердість поверхні, морфологія.